Available online at www.sciencedirect.com
ScienceDirect
Virology 375 (2008) 118–129
VIROLOGY
www.elsevier.com/locate/yviro

Mutation in murine coronavirus replication protein nsp4 alters assembly of double membrane vesicles

Mark A. Clementz [a,1], Amornrat Kanjanahaluethai [b,1], Timothy E. O'Brien [c], Susan C. Baker [a,*]

[a] Department of Microbiology and Immunology, Loyola University Stritch School of Medicine, Maywood, IL 60153 USA
[b] Department of Microbiology, Faculty of Medicine, Chiang Mai University, Chiang Mai, Thailand
[c] Department of Mathematics and Statistics, Loyola University, Chicago, IL 60626, USA

Received 29 October 2007; returned to author for revision 15 November 2007; accepted 12 January 2008
Available online 4 March 2008

Abstract

Coronaviruses are positive-strand RNA viruses that replicate in the cytoplasm of infected cells by generating a membrane-associated replicase complex. The replicase complex assembles on double membrane vesicles (DMVs). Here, we studied the role of a putative replicase anchor, nonstructural protein 4 (nsp4), in the assembly of murine coronavirus DMVs. We used reverse genetics to generate infectious clone viruses (icv) with an alanine substitution at nsp4 glycosylation site N176 or N237, or an asparagine to threonine substitution (nsp4-N258T), which is proposed to confer a temperature sensitive phenotype. We found that nsp4-N237A is lethal and nsp4-N258T generated a virus (designated Alb ts6 icv) that is temperature sensitive for viral replication. Analysis of Alb ts6 icv-infected cells revealed that there was a dramatic reduction in DMVs and that both nsp4 and nsp3 partially localized to mitochondria when cells were incubated at the non-permissive temperature. These results reveal a critical role of nsp4 in directing coronavirus DMV assembly.

Keywords: Coronavirus; Nonstructural proteins; Double membrane vesicles; ts mutant

Introduction

All positive-stranded RNA viruses that infect mammalian and plant hosts form membrane-associated replication complexes in the cytoplasm of infected cells (Salonen et al., 2005). Coronaviruses, such as mouse hepatitis virus (MHV) and severe acute respiratory syndrome coronavirus (SARS-CoV) that causes severe respiratory illness in humans (Peiris et al., 2004; Stadler et al., 2003), generate double membrane vesicles (DMVs), which are the sites of viral RNA synthesis (Baker and Denison, 2008; Goldsmith et al., 2004; Gosert et al., 2002; Snijder et al., 2006). The DMVs are generated by the association of coronavirus nonstructural proteins (nsps) with host intracellular membranes (Gosert et al., 2002; Harcourt et al., 2004; Prentice et al., 2004; Shi et al., 1999; Snijder et al., 2006). However, the role of each of the coronavirus nonstructural proteins in the assembly of DMVs is not yet clear.

The coronavirus nonstructural proteins are translated from the 5′-most gene of the genome, gene 1. Gene 1 contains two open reading frames (ORFs) that produce two large polyproteins, pp1a and pp1ab (Fig. 1A). Polyprotein 1a is processed by viral proteinases to generate intermediates and mature products nsp1-nsp11. Polyprotein 1ab is generated by a ribosomal frameshift between ORF1a and ORF1b and contains all 16 nsps (Masters, 2006; Ziebuhr and Snijder, 2007). For MHV, these large polyproteins undergo extensive proteolytic processing by three virally encoded proteinases, papain-like proteinase (PLP) 1, PLP2, and 3C-like proteinase (3CLpro) to produce intermediate and mature replicase proteins (Baker et al., 1989; Bonilla et al., 1997; Bost et al., 2000; Denison et al., 1995; Graham and Denison, 2006; Kanjanahaluethai and

* Corresponding author. Department of Microbiology and Immunology, Loyola University Chicago, Stritch School of Medicine, 2160 South First Avenue, Building 105 Room 3929, Maywood, IL 60153, USA. Fax: +1 708 216 9574.
E-mail address: sbaker1@lumc.edu (S.C. Baker).
[1] These authors contributed equally to this work.

0042-6822/$ - see front matter © 2008 Elsevier Inc. All rights reserved.
doi:10.1016/j.virol.2008.01.018

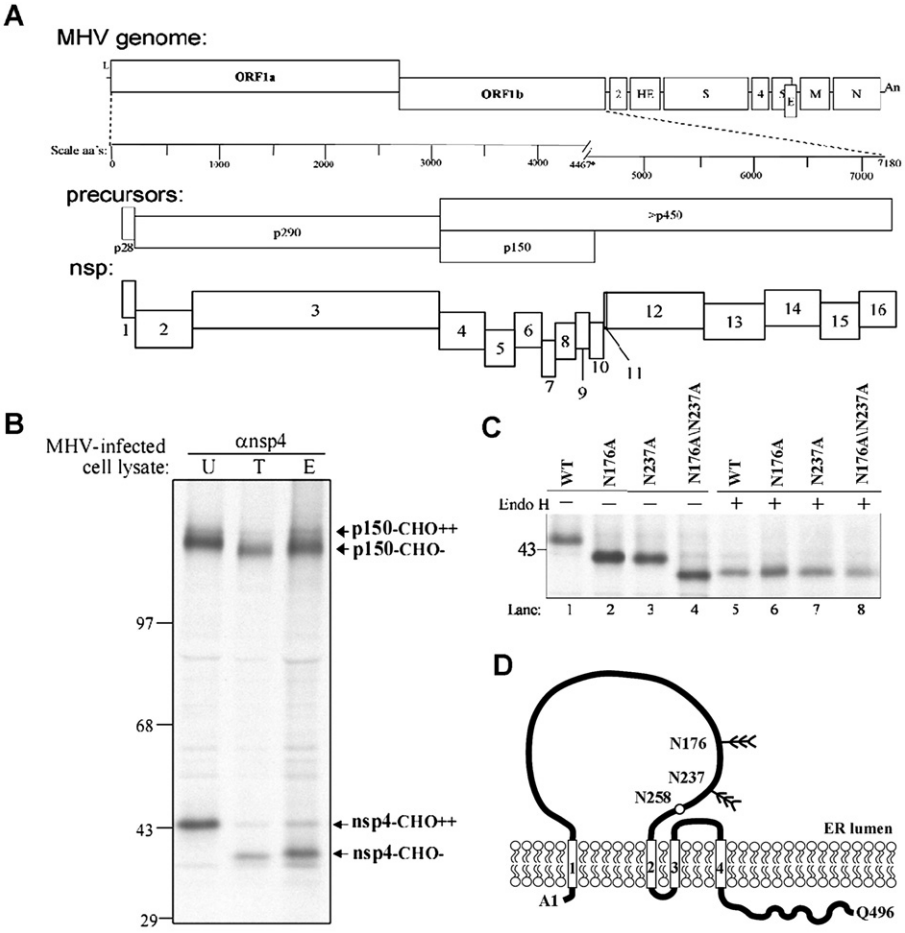

Fig. 1. MHV replicase highlighting predicted nsp4 topology and analysis of N-linked glycosylation. (A) The first two-thirds of the MHV genome (ORF 1a and ORF 1b) encode the viral replicase proteins. The nonstructural proteins (nsps) are synthesized as polyproteins processed into precursors then 16 mature replicase products. (B) Analysis of p150 and nsp4 after tunicamycin and endo H treatments. HeLa-MHVR cells were infected with MHV-JHM, untreated (U) or treated with 1 μg/ml of tunicamycin (T) for 1 h prior to and during labeling. Endo H treatment (E) was performed after immunoprecipitation with α-nsp4. (C) HeLa-MHVR cells were infected with vTF7.3, and co-transfected with plasmids encoding PLP2 and substrate encoding either WT or mutant nsp4. Proteins were radiolabeled (^{35}S-*trans*-label) and immunoprecipitated with α-nsp4 antibodies. IP products were untreated or treated with endo H, separated on 5–10% gradient SDS-PAGE gel, and visualized by autoradiography. (D) Predicted topology of nsp4 indicating the location of two glycosylation sites and a ts lesion within the luminal loop.

Baker, 2001; Kanjanahaluethai et al., 2003; Lu et al., 1998, 1995; Schiller et al., 1998). The replicase intermediate p150 contains the mature products nsp4-nsp11 and has been proposed to be functional in the synthesis of negative strand RNA and/or as a scaffold for the assembly of the transcriptase/replicase complex (Kanjanahaluethai and Baker, 2000; Sawicki et al., 2007, 2005).

Bioinformatic analysis indicates that the replicase products nsp3, nsp4, and nsp6 have membrane spanning helices (Ziebuhr et al., 2000). Biochemical fractionation studies have shown that nsp3 and nsp4 are integral membrane glycoproteins (Gosert et al., 2002; Kanjanahaluethai et al., 2007; Oostra et al., 2007). Recently, Sparks et al. (2007) showed that the amino terminal region of nsp4 is essential for viral replication as deletions in this region are lethal. Furthermore, Sawicki et al. (2005) sequenced a large panel of temperature sensitive (ts) mutants of MHV and identified one ts mutant, Alb ts6, that contained a substitution of asparagine to threonine at amino acid position 258 within the amino terminal region of nsp4. This mutation was predicted to confer the RNA minus ts phenotype, but how this mutation affects MHV RNA synthesis is not yet understood.

To investigate the role of specific asparagine residues within the amino terminal domain of nsp4 in MHV replication, we engineered amino acid substitutions at putative glycosylation sites nsp4-N176 and nsp4-N237 and the putative ts lesion nsp4-N258 and isolated infectious clone virus (icv). We found that nsp4-N176 and nsp4-N237 are glycosylated and that substitution of nsp4-N237 to alanine was lethal for virus replication, whereas substitution of nsp4-N176 to alanine had no effect on virus replication. Our results show that the asparagine to threonine substitution at nsp4-258 was sufficient to bestow a ts phenotype, and this virus was designated Alb ts6 icv. We found that proteolytic processing of p150 is unaffected in the Alb ts6 icv at either temperature. However, at the non-permissive temperature, DMV assembly and mitochondria morphology are disrupted in Alb ts6 icv-infected cells and viral replicase proteins partially localize with mitochondria. These data demonstrate that nsp4 is an important factor in DMV assembly and are consistent with the

hypothesis that nsp4 is an anchor or scaffold for the replication complex.

Results

MHV replicase precursor p150 and product nsp4 are modified by N-linked glycosylation

Previous studies indicated that MHV nsp4 is a glycoprotein (Oostra et al., 2007), but it was unclear if the p150 precursor was also modified. To determine if both the precursor p150 and the mature product nsp4 are modified by N-linked glycosylation, we analyzed these proteins for sensitivity to tunicamycin and endoglycosidase H (endo H). MHV-infected cells were radiolabeled with ^{35}S-*trans*-label and either mock-treated or treated with tunicamycin and lysates and were subjected to immunoprecipitation with anti-nsp4 and then treated with endo H. We found that both the precursor p150 and the mature product nsp4 were modified by N-linked glycosylation and that these modifications were sensitive to endo H, indicating that these proteins did not progress past the endoplasmic reticulum (ER) (Fig. 1B).

Bioinformatic analysis indicated that nsp4 residues N176 and N237 are consensus sites for N-linked glycosylation (consensus sequence: NXS/T). To determine if nsp4-N176 and nsp4-N237 are specifically modified by N-linked glycosylation, a cDNA clone [MHV-Cen-nsp4 (Kanjanahaluethai and Baker, 2000)] expressing the entire nsp4 region and the cleavage site recognized by PLP2, was subjected to site-directed mutagenesis to generate alanine substitutions at these sites, and the mobility of WT and mutant forms of nsp4 was assessed by SDS-PAGE. Cells were transfected with constructs expressing pPLP2 (proteinase) and either WT or mutant forms of pCen-nsp4 DNA (substrate) and newly synthesized proteins were radiolabeled with ^{35}S-*trans*-label. Cell lysates were prepared and subjected to immunoprecipitation with an α-nsp4 antibody to detect the mature form of nsp4 generated by cleavage of Cen-nsp4 by PLP2. The immunoprecipitated nsp4 was either mock-treated or endo H treated and electrophoretic mobility of protein was assessed. As seen in Fig. 1C, nsp4 encoding either the N176A or N237A substitutions exhibited faster migration as compared to WT nsp4. The nsp4-N176A/N237A double mutant migrated faster than either single mutant. For products treated with endo H, which cleaves N-linked oligosaccharides, the mobility of all four proteins was similar to that of the nsp4-N176A/N237A double mutant, as expected. These data indicate that nsp4-N176 and nsp4-N237 are in fact subjected to N-linked glycosylation.

Recent studies have suggested that an asparagine residue in the luminal domain of nsp4 is important for MHV RNA synthesis. Sawicki et al. (2005) analyzed a series of MHV temperature sensitive mutants that do not make viral RNA at the non-permissive temperature. They identified one virus, designated as Alb ts6, with an asparagine to threonine substitution at nsp4 residue 258. This residue was implicated as the site responsible for temperature sensitive defect. However, the mechanism by which this substitution in nsp4 causes the defect in RNA synthesis in Alb ts6 is not known. A schematic diagram

Table 1
Primers used for engineering icv mutants, RT-PCR, and sequencing

Primer	Sequence (5′-3′)	Nucleotides[a]	Sense	Purpose
A59-4	TCTTAATAGCGGCCAACACC	10991–11010	−	RT-PCR
A59-18	CATGAATGGTCTGCTGCATT	8003–8022	+	RT-PCR/Sequencing Clone B
A59-CS1	GTGGCAATGGCAAGAGG	5411–5427	+	Sequencing Clone B
A59-DS1	CATGTACAGGCTAATGTTG	8523–8541	+	Sequencing Clone B
A59-3	TGTTAACTTCCGCTCCTGCT	5066–5085	+	Sequencing Clone B
MAC-3	CTCGCTCTATGACCTACTGC	9361–9380	+	Sequencing Clone B
MAC-4	CAGTCCAGTTACGCTGGAGTC	pSMART vector	+	Sequencing Clone B
MAC-5	AACTGCCCGACGATGTTG	5773–5790	+	Sequencing Clone B
MAC-6	TGTGGTGTTGGCTAGTGATG	6224–6243	+	Sequencing Clone B
MAC-7	GCTGCTGATGTCAAAGAGG	6567–6585	+	Sequencing Clone B
MAC-8	TGCCTGCTATTGTGCTGTG	6887–6905	+	Sequencing Clone B
MAC-9	CGTTTGTGGGACAGATAG	7165–7182	+	Sequencing Clone B
MAC-10	CATTGGAGTGCTCGTTTG	7518–7535	+	Sequencing Clone B
B-MUT	AACCCATGCATTTGCTACTG	9080–9099	+	Sequencing Clone B
B285-JHM	GGGTGTTATGCATGCTGCTTCTCTGTATAG	9247–9276	+	nsp4-N176A pCen-nsp4
B286-JHM	CTATACAGAGAAGCAGCATGCATAACACCC	9247–9276	−	nsp4-N176A pCen-nsp4
B287-JHM	ATTTGTTTTAATTTTGCTAGTTCATGGGTACTG	9428–9460	+	nsp4-N237A pCen-nsp4
B288-JHM	CAGTACCCATGAACTAGCAAAATTAAAACAAAT	9428–9460	−	nsp4-N237A pCen-nsp4
B285-A59	GGGTGTTATGCACGCTGCCTCTCTGTATAG	9233–9262	+	nsp4-N176A Clone B
B286-A59	CTATACAGAGAGGCAGCGTGCATAACACCC	9233–9262	−	nsp4-N176A Clone B
B287-A59	ATCTGCTTTAATTTTGCTCGTTCATGGGTATTG	9414–9446	+	nsp4-N237A Clone B
B288-A59	CAATACCCATGAACGAGCAAAATTAAAGCAGAT	9414–9446	−	nsp4-N237A Clone B
MAC-1	GTGGTAGGACAGCTTTTGATTTAATACATC	9484–9513	+	nsp4-N258T Clone B
MAC-2	CAAAAGCTGTCCTACCACAAAAAGTTCCAG	9472–9501	−	nsp4-N258T Clone B

[a] Numbering according to MHV-A59 GenBank accession number NC001846 or MHV-JHM GenBank accession number NC006852. The underlined nucleotides indicate the mutated nucleotides.

of nsp4 topology indicating the position of the two asparagine residues modified by N-linked glycosylation, and an asparagine to threonine change predicted to be responsible for the temperature sensitive phenotype are depicted in Fig. 1D.

Generating infectious clone viruses with amino acid substitutions in nsp4

To determine if nsp4-N176, nsp4-N237, or nsp4-N258 is important for nsp4 function, we generated virus encoding each specific substitution. Each substitution was introduced into the MHV-A59 genome using a reverse genetics approach pioneered by Yount et al. (2002) as described in the Materials and methods. Briefly, PCR based site-directed mutagenesis was performed on the plasmid DNA containing the region of nsp4 to be mutated (Clone B) using specific primers (Table 1). Each mutant clone B DNA fragment was ligated with the remaining six WT fragments to produce full-length MHV cDNA which was then in vitro transcribed using T7 RNA polymerase. Infectious RNA was electroporated into BHK-MHVR cells and cells were laid over a semi-confluent monolayer of DBT cells. Cells were incubated at 33 °C and scored for cytopathic effect. Supernatant from cells showing syncytia formation was collected and passaged over a fresh monolayer of DBT cells to generate a stock of infectious clone virus. RNA was isolated from mock and icv-infected DBT cells and RT-PCR was performed to amplify the region containing the mutation of interest. Amplicons were sequenced to verify the presence of the engineered mutation (Fig. 2). Infectious viruses were successfully obtained for position N176A (referred to as nsp4-N176A icv) and N258T (designated Alb ts6 icv). However, we were unable to generate the nsp4-N237A single or nsp4-N176A/N237A double mutant virus, which indicates that mutation of N237 may be lethal for nsp4 function.

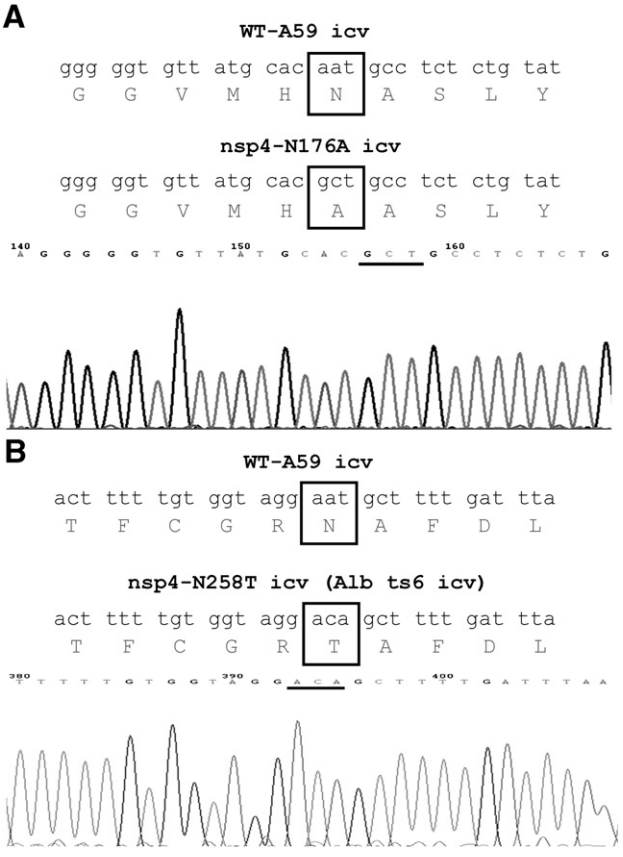

Fig. 2. Sequence analysis of mutant infectious clone virus. DBT cells were infected with WT-A59 icv, nsp4-N176A icv, or Alb ts6 icv and at 12 h.p.i. RNA was isolated. RT-PCR was performed on viral RNA using primers listed in Table 1, and PCR products were sequenced across the nsp4 region.

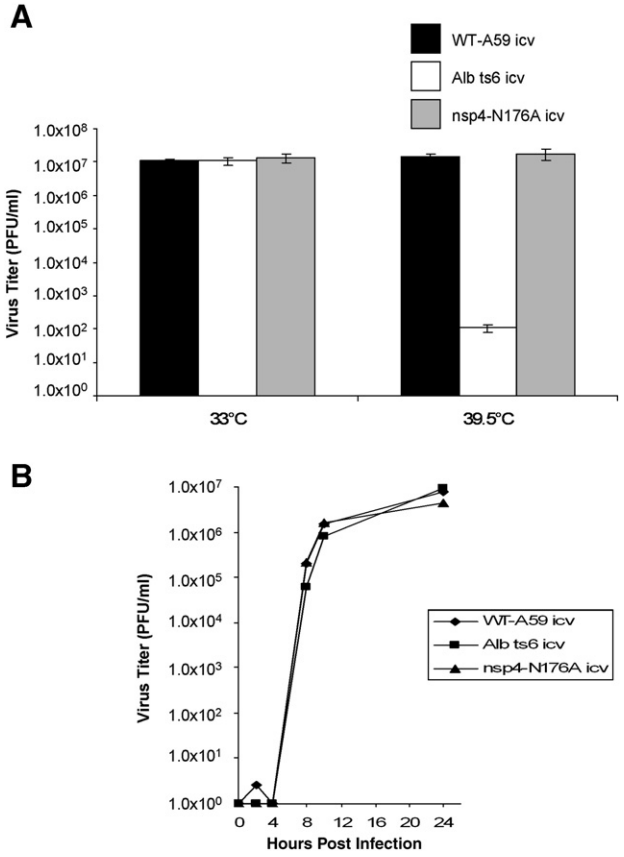

Fig. 3. Growth characteristics of infectious clone viruses. (A) Titer of WT-A59 icv, Alb ts6 icv, and nsp4-N176A icv following infection at the permissive or nonpermissive temperature for 15 hours, when supernatant was harvested and virus titrated at 33 °C. Plaques were counted 48 h.p.i. Black bars, WT-A59 icv; white bars, Alb ts6 icv; gray bars, nsp4-N176A icv. Viral titers were performed in triplicate; error bars indicate standard deviation from the mean. (B) One-step growth curve of WT-A59 icv, Alb ts6 icv, and nsp4-N176A icv at the permissive temperature of 33 °C. Supernatant was collected at the indicated time points and viral titer was determined by plaque assay.

Analysis of the ts phenotype in nsp4-mutant MHV icv

To determine if either Alb ts6 icv or nsp4-N176A icv is temperature sensitive, we measured the amount of infectious particles produced by virus-infected cells incubated at the permissive (33 °C) or non-permissive (39.5 °C) temperature and titrated at the permissive temperature. Two sets of DBT cells were infected with WT-A59 icv, Alb ts6 icv, or nsp4-N176A icv at an MOI of 0.1. One set of infected cells was maintained at the

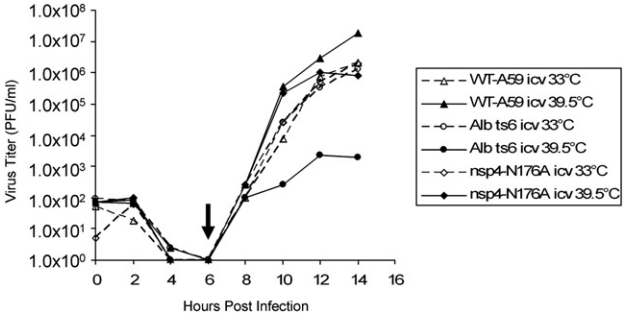

Fig. 4. Temperature shift assay on infectious clone virus. Two sets of DBT cells were infected with WT-A59 icv, Alb ts6 icv, or nsp4-N176A icv at an MOI of 0.1 and incubated at 33 °C. At 6 h.p.i., one set of infected cells was shifted to 39.5 °C. Supernatant was harvested at two hour intervals and virus production was measured by plaque assay. Arrow indicates time of temperature shift.

permissive temperature of 33 °C, while the other was incubated at the non-permissive temperature of 39.5 °C. At 15 h.p.i., cell-free supernatant was collected. Ten-fold serial dilutions (in triplicate) of isolated supernatant were used to infect DBT cells incubated at the permissive temperature. After 48 h, plaques were counted and viral titer was determined. WT-A59 icv replicated to high titers of 1.08×10^7 plaque forming units (PFU)/ml at 33 °C and 1.42×10^7 PFU/ml at 39.5 °C. nsp4-N176A icv also produced a similar size of plaques and reached titers of 1.33×10^7 PFU/ml at 33 °C and 1.75×10^7 PFU/ml at 39.5 °C. The Alb ts6 icv replicated efficiently at 33 °C (1.08×10^7 PFU/ml), but replication was dramatically reduced at 39.5 °C (4.08×10^2 PFU/ml) (Fig. 3A). One-step growth curve analysis was then performed on WT-A59 icv, Alb ts6 icv, and nsp4-N176A icv. DBT cells were infected with icv at a multiplicity of infection of 0.1, incubated at the permissive temperature, and production of infectious virus was monitored by plaque assay. As shown in Fig. 3B, when grown at 33 °C, WT-A59 icv, Alb ts6 icv, and nsp4-N176A icv all replicated with indistinguishable kinetics.

Temperature shift experiments were then performed to further assess the ts phenotype. Two sets of DBT cells were infected with WT-A59 icv, Alb ts6 icv, or nsp4-N176A icv at an MOI of 0.1 and incubated at 33 °C. At 6 h.p.i., one set of infected cells was shifted to 39.5 °C. Supernatant was harvested at two hour intervals and virus production was measured by plaque assay. As depicted in Fig. 4, WT-A59 icv, nsp4-N176A icv, and Alb ts6 icv at 33 °C grew to similar titers and statistical analysis revealed that all icvs exhibited a common growth curve ($p=0.9459$). At 39.5 °C however, Alb ts6 icv titers fell over 3 logs by 12–14 h.p.i. as compared to WT-A59 icv or nsp4-N176A icv, and Alb ts6 icv exhibited distinct growth kinetics ($p<0.0001$). Taken together, these data indicate that the N258T mutation in nsp4 is sufficient to confer a ts phenotype to the Alb ts6 icv.

Analysis of proteolytic processing of p150 in the Alb ts6 icv and nsp4-N176A icv

One possible explanation for the ts phenotype of the Alb ts6 icv is that nsp4 processing is altered at the non-permissive temperature. To address this issue, DBT cells were infected with WT-A59 icv, Alb ts6 icv, and nsp4-N176A icv at an MOI of 1.0 and at 4 h.p.i. radiolabeled with ^{35}S-*trans*-label for 2 h. At 6 h.p.i., cell lysates were prepared and subjected to immunoprecipitation with nsp-specific antibodies. As seen in Figs. 5A–D, a large precursor of 150 kDa is detected from which the mature nsp4-nsp10/11 products are generated (Kanjanahaluethai and Baker, 2000). The liberation of nsp4 was detected in cells infected with WT-A59 icv, Alb ts6 icv, or nsp4-N176A icv virus at both the permissive and non-permissive temperature. The mobility of nsp4 in the nsp4-N176A icv was increased, which is consistent with the absence of glycosylation at amino acid 176 (Fig. 5A). The processing of nsp5, nsp8, nsp9, and nsp10 was also unaffected in cells infected with WT-A59 icv, Alb ts6 icv, or nsp4-N176A icv at both temperatures (Figs. 5B–D). Overall, these results indicate that the ts phenotype is not due to any alteration in the processing of nsp4 or other p150-derived replicase products.

Ultra-structural analysis of DMV assembly in icv-infected cells

We hypothesize that nsp4 is a key anchor for DMV assembly and therefore asked if the formation of DMVs was altered

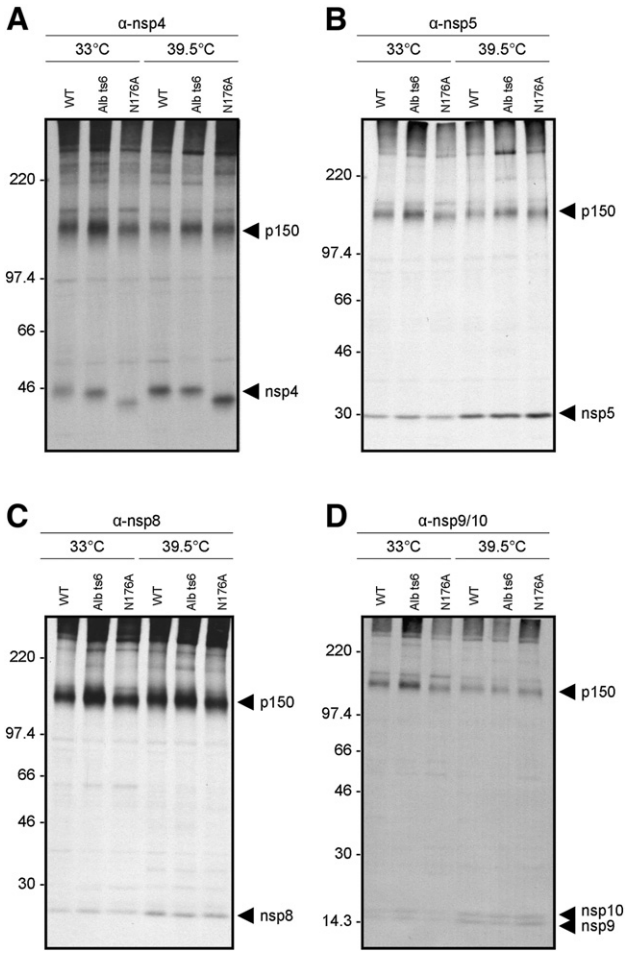

Fig. 5. Proteolytic processing of infectious clone virus. DBT cells were infected with WT-A59 icv, Alb ts6 icv and nsp4-N176A icv, at 4 h.p.i. radiolabeled with ^{35}S-*trans*-label for 2 h, and at 6 h.p.i. cell lysates were prepared and subjected to immunoprecipitation with (A) α-nsp4, (B) α-nsp5, (C) α-nsp8, and (D) α-nsp9/10. All replicase antibodies also detect the p150 precursor.

in cells infected with the Alb ts6 icv incubated at the non-permissive temperature. We assessed DMV formation by transmission electron microscopy (TEM) analysis to determine if the reported defect in RNA synthesis is due to a defect in DMV assembly. Two sets of DBT cells were infected with WT-A59 icv or Alb ts6 icv at an MOI of 1.0 and incubated at 33 °C. At 3.5 h.p.i., one set of infected cells was shifted to 39.5 °C. At 5.5 h.p.i., cells were harvested and processed for TEM analysis. DMVs can be visualized by TEM as darkly ringed vesicles in the cytoplasm of MHV-infected cells (Gosert et al., 2002). As shown in Fig. 6, DMV formation induced by WT-A59 icv was similar at both permissive and non-permissive temperatures. At 33 °C, the Alb ts6 icv induced DMV formation comparable to WT-A59 icv; however, at the non-permissive temperature of 39.5 °C, the Alb ts6 icv produced fewer DMVs. The most striking feature we observed was that the morphology of the mitochondria was altered in cells infected with the Alb ts6 icv incubated at 39.5 °C. As seen in Fig. 6D, the mitochondria were larger and extensively vacuolated. The overall reduction in DMVs and the striking change in mitochondrial morphology lead us to hypothesize that the mutation in nsp4 resulted in altered localization of nsp4 and potentially other MHV replicase products, resulting in a block in viral RNA synthesis.

Co-localization of MHV replicase proteins with mitochondria

The abnormalities observed in the mitochondria of cells infected with Alb ts6 icv incubated at the non-permissive temperature led us to explore whether MHV replicase proteins,

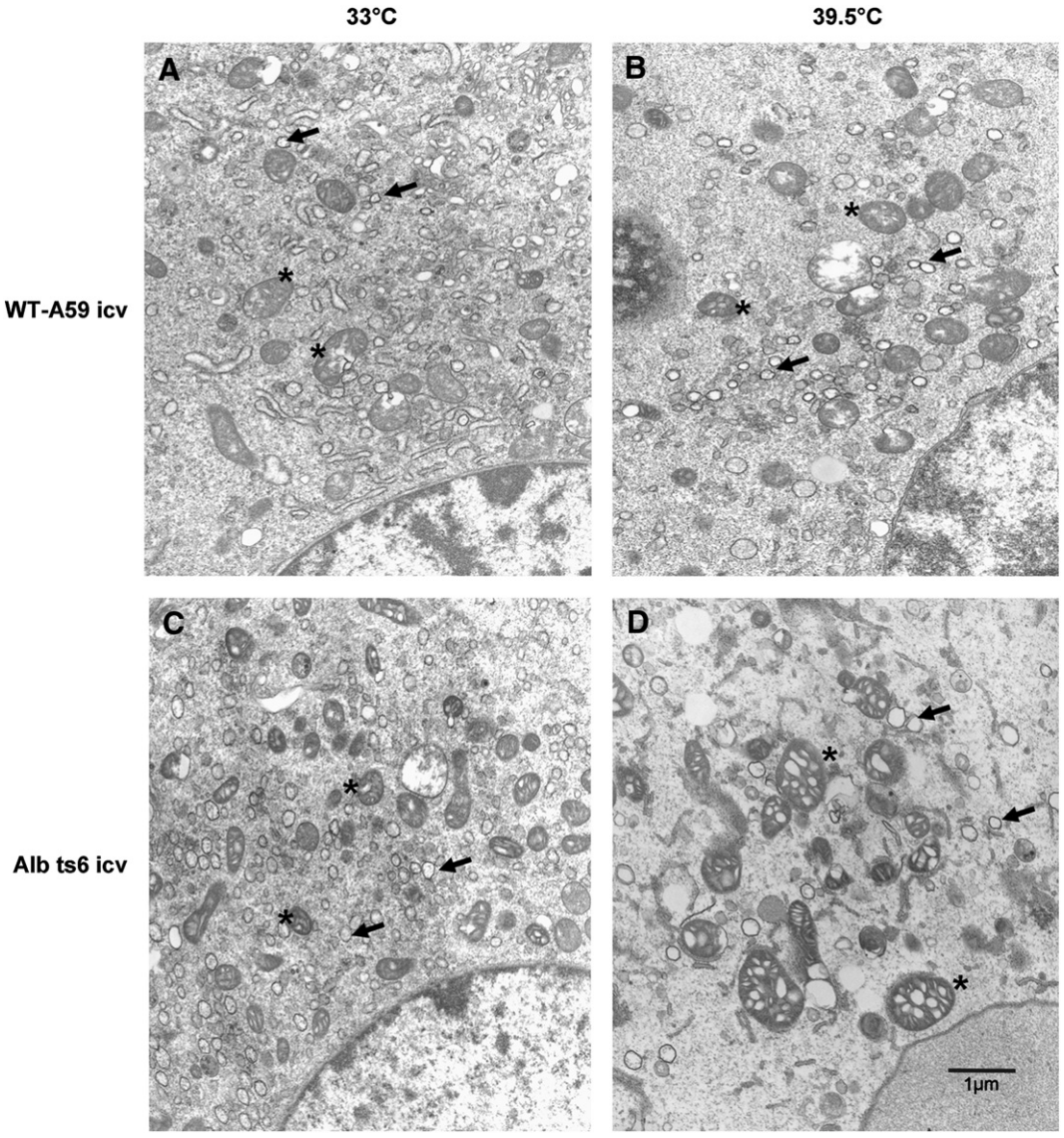

Fig. 6. TEM analysis of DMV formation by the WT-A59 icv and Alb ts6 icv at the permissive and non-permissive temperatures. Two sets of DBT cells were infected with WT-A59 icv or Alb ts6 icv at an MOI of 1.0 and incubated at 33 °C (A and C). At 3.5 h.p.i., one set of infected cells (B and D) was shifted to 39.5 °C. At 5.5 h.p.i., cells were harvested and processed for TEM analysis. DMVs can be visualized by TEM as darkly ringed vesicles in the cytoplasm of MHV-infected cells indicated by the arrows. Asterisks denote mitochondria. Scale bar equals 1 μm.

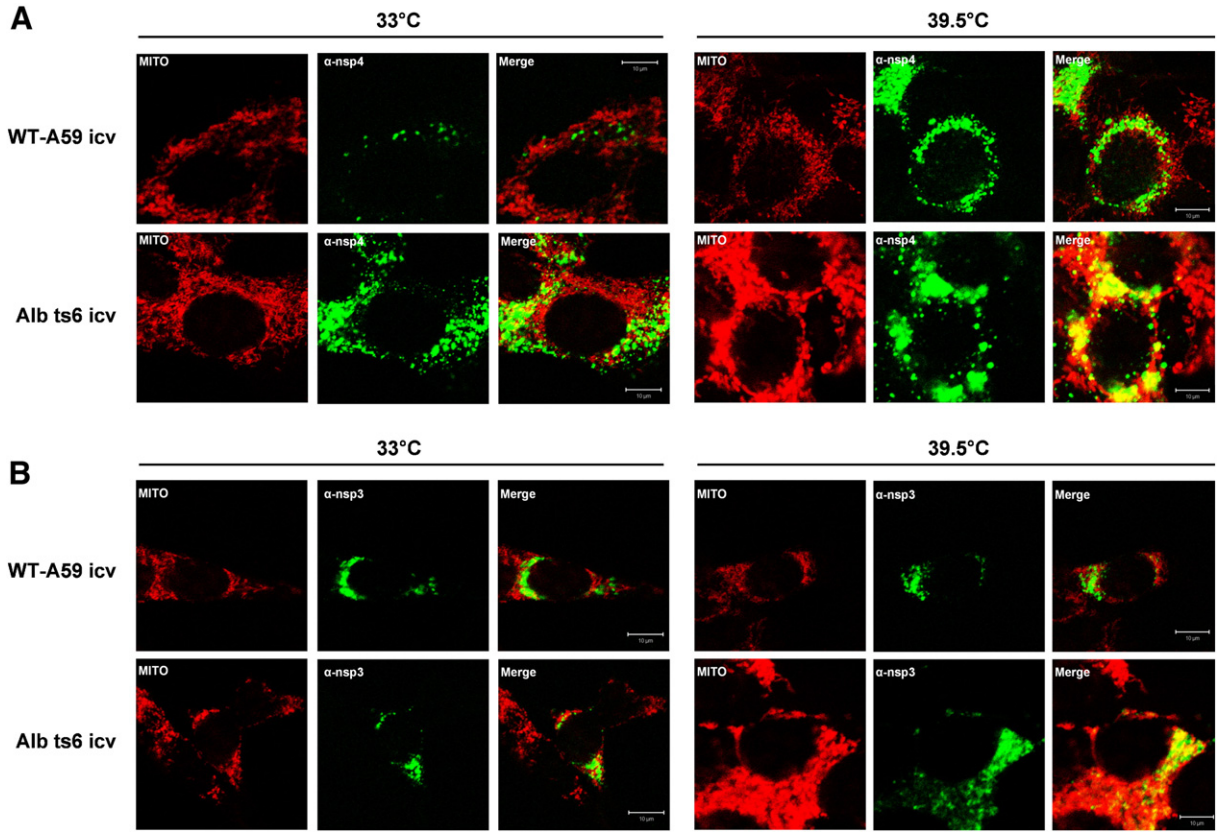

Fig. 7. Localization of MHV replicase proteins and a mitochondrial marker in DBT cells infected with WT-A59 icv and Alb ts6 icv. Two sets of DBT cells were infected with WT-A59 icv or Alb ts6 icv at an MOI of 1.0 and incubated at 33 °C. At 3.5 h.p.i., one set of infected cells was shifted to 39.5 °C. At 5 h.p.i. cells were labeled with MitoTracker Red fluorescent dye. At 5.5 h.p.i., cells were harvested, fixed, and permeabilized for immunofluorescence assays. Permeabilized cells were then incubated with antibodies to either nsp4 (A) or nsp3 (B). Scale bar equals 10 μm.

which normally co-localize with ER in DBT cells (Shi et al., 1999), were co-localizing with mitochondria. Two sets of DBT cells were infected with WT-A59 icv or Alb ts6 icv at an MOI of 1.0 and incubated at 33 °C. At 3.5 h.p.i., one set of infected cells was shifted to 39.5 °C. At 5 h.p.i., cells were labeled with MitoTracker Red fluorescent dye, which is concentrated by active mitochondria. At 5.5 h.p.i., cells were harvested, fixed, and permeabilized for immunofluorescence assays. Permeabilized cells were then incubated with antibodies to either nsp3 or nsp4. As shown in Fig. 7A, staining for nsp4 (green) and mitochondria (red) was non-overlapping in cells infected with WT-A59 icv at either temperature. At the permissive temperature, Alb ts6 icv nsp4 and mitochondria displayed a very slight increase in co-localization versus WT-A59 icv. At 39.5 °C however, co-localization of nsp4 and mitochondria was substantially increased. The intensity of the red signal was also increased in cells infected with Alb ts6 icv at the non-permissive temperature, which may reflect the increased in size of the mitochondria that we observed by TEM. Similar results were obtained in three independent experiments, with extensive co-localization detected only in the Alb ts6 icv-infected cells incubated at the non-permissive temperature.

To extend these findings, we performed similar experiments using HeLa cells stably transfected with the MHV receptor (MHVR). Two sets of HeLa-MHVR cells were infected with WT-A59 icv or Alb ts6 icv at an MOI of 1.0 and incubated at 33 °C. At 3.5 h.p.i., one set of infected cells was shifted to 39.5 °C. At 5 h.p.i., mitochondria were labeled with MitoTracker Red fluorescent dye or following fixation with an antibody to pyruvate dehydrogenase (PDH), which is a mitochondrial matrix protein. Antibodies against nsp3 and nsp4 were again used to detect replicase products. As seen in Fig. 8, extensive overlap between replicase proteins nsp3 and nsp4 and mitochondria was detected only in the Alb ts6 icv-infected cells incubated at the non-permissive temperature (39.5 °C). Similar results were obtained with MitoTracker stained HeLa-MHVR cells and MitoTracker and PDH were found to completely overlap (data not shown). These results are consistent with the TEM studies and reveal that the mutant form of nsp4 is partially localized to mitochondria at the non-permissive temperature. Furthermore, we also detected co-localization with mitochondria using the α-nsp3 antibody in Alb ts6 icv-infected cells incubated at 39.5 °C (Figs. 7B and 8B). Importantly, nsp3, and perhaps other replicase products, are misdirected due to nsp4 mis-localization and are likely unable to efficiently assemble into functional DMVs in the Alb ts6 icv-infected cells. This inability to generate functional DMVs and/or replication complexes would lead to an inability to synthesize viral RNA,

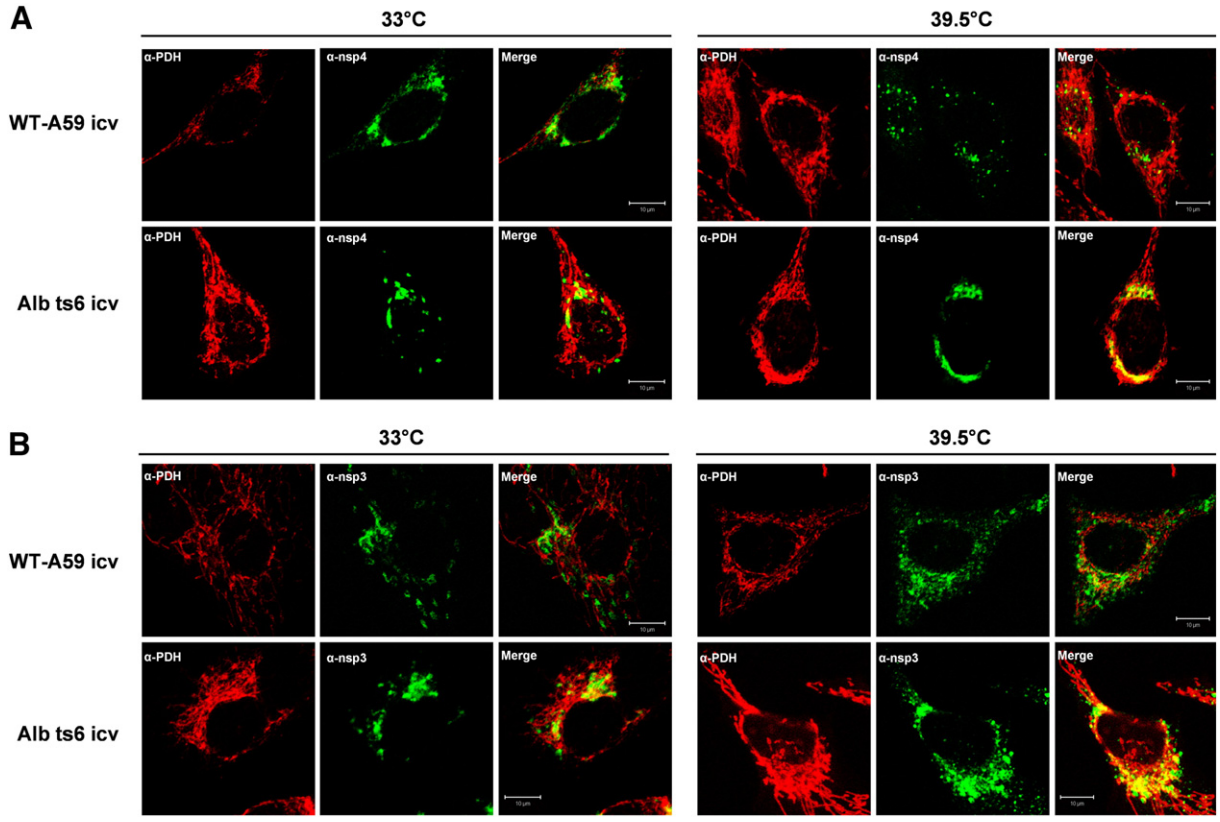

Fig. 8. MHV replicase protein localization in icv-infected HeLa-MHVR cells using antibodies to the mitochondrial protein pyruvate dehydrogenase (PDH). Two sets of HELA-MHVR cells were infected with WT-A59 icv or Alb ts6 icv at an MOI of 1.0 and incubated at 33 °C. At 3.5 h.p.i., one set of infected cells was shifted to 39.5 °C. At 5.5 h.p.i., cells were harvested, fixed, and permeabilized for immunofluorescence assays. Permeabilized cells were then incubated with antibodies to PDH and either nsp4 (A) or nsp3 (B). Scale bar equals 10 μm.

which is the reported phenotype of Alb ts6 (Sawicki et al., 2005).

Discussion

Positive-strand RNA viruses express viral replicase proteins that must interact with host intracellular membranes to create an environment for optimal viral RNA synthesis. Coronaviruses express replicase proteins that assemble to generate DMVs in the cytoplasm of infected cells (Goldsmith et al., 2004; Gosert et al., 2002; Snijder et al., 2006). In this study, we investigated the role of one coronavirus replicase product, nsp4, in MHV replication. Because nsp4 is a transmembrane protein, we hypothesize that nsp4 is critical for assembly of the replication complex on DMVs. To test this hypothesis, we generated viruses with specific amino acid substitutions in nsp4 and assessed the effect of these substitutions on viral replication.

First, we investigated the role of two putative N-linked glycosylation sites in MHV replication. Using endo H assays, we found that both the nsp4-11 precursor (p150) and the nsp4 product are modified by N-linked glycosylation (Fig. 1B). We engineered alanine substitutions (nsp4-N176A and nsp4-N237A) into WT-A59 virus and found that nsp4-N176A icv behaved identically to WT-A59 icv suggesting that glycosylation at this site is not required for MHV replication. However, we were unable to generate either nsp4-N237A icv or nsp4-N176A/N237A (double glycosylation knockout) icv suggesting that glycosylation of nsp4-N237A, or specific folding of nsp4 in this luminal domain, is required for MHV replication.

Next, we investigated the role of nsp4-N258 in MHV replication. Sawicki et al. (2005) analyzed the sequence of 19 MHV ts mutants and reported that one of these mutant viruses, Alb ts6, encoded a substitution of asparagine for threonine at nsp4-258. They hypothesized that this mutation alone was sufficient to confer the ts and RNA synthesis-negative phenotype to MHV-A59. Via reverse genetics, we engineered the nsp4-N258T mutation into MHV and designated this virus as Alb ts6 icv. We found that the nsp4-N258T substitution was indeed sufficient to induce temperature sensitivity. Alb ts6 icv titers were reduced approximately 5 orders of magnitude when incubated at the non-permissive temperature; however, Alb ts6 icv titers at 33 °C were comparable to WT-A59 icv (Fig. 3A). Growth kinetics, assayed by a one-step growth curve at the permissive temperature, were indistinguishable between Alb ts6 icv and WT-A59 icv. However, temperature shift experiments revealed that upon incubation at the non-permissive temperature, Alb ts6 icv titers fell 1000 fold (Fig. 4).

Using a similar reverse genetics approach, Donaldson et al. (2007) found that a single amino acid substitution in nsp10 conferred temperature sensitivity to the icTS-LA6 virus. This

analysis revealed that nsp10 is a necessary cofactor for 3CLpro activity as proteolytic processing of the replicase intermediate p150 was defective in icTS-LA6-infected cells incubated at the non-permissive temperature. In contrast, we found that Alb ts6 icv had no defects in proteolytic processing when virus-infected cells were incubated at the non-permissive temperature (Fig. 5). An alternative explanation for the RNA minus ts phenotype of Alb ts6 is that a mutation in nsp4 affects assembly of DMVs. To test this hypothesis, we performed TEM analysis of Alb ts6 icv-infected cells. This analysis revealed that DMV assembly is severely impaired in the Alb ts6 icv-infected cells incubated at the non-permissive temperature (Fig. 6D). The failure to assemble DMVs, which are necessary for viral RNA synthesis, is consistent with the RNA minus phenotype observed by Sawicki et al. (2005). Our results demonstrate that nsp4 plays a critical role in the formation and/or maintenance of DMVs.

Also, TEM analysis of Alb ts6 icv-infected cells incubated at the non-permissive temperature showed a disruption of mitochondrial morphology; the mitochondria were enlarged and extensively vacuolated (Fig. 6D). Using confocal microscopy, we assessed whether nsp4-N258T was localized to the mitochondria. We found that nsp4-N258T partially co-localized with mitochondria in virus-infected cells incubated at the non-permissive temperature (Figs. 7A and 8A). Interestingly, we found that replicase product nsp3 also co-localized with mitochondria, suggesting that nsp4-N258T may direct the localization of other replicase components (Figs. 7B and 8B). Currently, it is unclear if a replicase precursor or only the final replicase products are directed to specific membrane sites or if nsp4 is actually penetrating the mitochondrial membrane. Since nsp4 is an integral membrane protein originally derived from the ER, the co-localization detected may be due to membrane reorganization. DMVs are likely diffusible in the cytoplasm and perhaps nsp4-N258T is directing the localization of DMVs to mitochondria where they are sequestered or fused with mitochondrial membranes. Further experiments will be required to address this important issue.

The aberrant mitochondrial morphology and partial co-localization with nsp3 and nsp3 raises questions about the role for mitochondria in MHV replication. Could nsp4-N258T be localizing to mitochondria in error resulting in reduced DMV assembly? Or is there a mitochondrial phase in MHV replication whose progression is inhibited by the nsp4-N258T substitution? Previous studies demonstrate that for some viruses, the replicase complex can be directed to use different membrane sources for efficient virus replication. For example, Flock house virus (FHV) normally induces spherules within the outer membrane of the mitochondria providing precedence for the use of mitochondrial membranes as the site of membrane-bound replication complex assembly (Kopek et al., 2007; Miller and Ahlquist, 2002; Miller et al., 2001). To determine if mitochondrial membranes were required for replication, Miller et al. (2003) replaced the mitochondrial outer membrane targeting signal of FHV protein-A with that of an ER targeting signal and measured viral replication. They found that the ER-targeted replication complex functioned as efficiently, if not more efficiently, than the normal mitochondria-targeted replication complex. Therefore, a specific source of membranes for replication complex assembly is not required for FHV. For MHV, it is unclear if the replication complex could be appropriately targeted to mitochondria, or if cytoplasmic DMVs are critical for MHV replication. In addition, it will be interesting to determine if WT nsp4 or nsp4-N258T expressed in *trans* can direct MHV replication complexes to specific membrane sites.

Complementation studies are useful for identifying products which can act in *trans* to provide a functional protein for a defective gene product. Complementation analyses have been done with a large panel of ts mutants within the MHV replicase and have provided insights into the functions of intermediate and fully processed replicase proteins (Baric et al., 1990; Donaldson et al., 2007; Fu and Baric, 1994; Sawicki et al., 2005; Schaad et al., 1990; Siddell et al., 2001; Younker and Sawicki, 1998). Interestingly, although MHV ORF1a encodes eleven mature nsps, mutants within ORF1a do not complement each other. There are at least two possible explanations for these results: 1) a polyprotein precursor, such as p150, may function itself, or function in *cis* and therefore cannot be complemented by mature nsp products (Deming et al., 2007; Sawicki et al., 2005); and 2) mutations in one nsp may affect the production, function or localization of multiple products and therefore cannot be complemented by a *trans*-acting factor. For example, virus with a mutation in nsp10 (TS-LA6) crossed with a nsp4 mutant (Alb ts6) do not complement each other (Sawicki et al., 2005). Donaldson et al. (2007) suggest that the icTS-LA6, which exhibits a processing defect, fails to complement due to the inability to generate mature forms of nsp4-nsp16. Thus, a mutation in a single nsp (nsp10) affects the production of several nsps (nsp4-nsp16). Likewise, the mutation analyzed in this study, nsp4-N258T, which results in defects in DMV assembly and localization, also affects the localization of other nsps, such as nsp3. Therefore, like the icTS-LA6, the defect in Alb ts6 icv induces an overarching defect in MHV replication. These observations highlight the complex nature of coronavirus replication complex assembly and maturation and indicate that interplay among partially and fully processed replicase products ultimately leads to competent replication complexes.

The results presented in this study indicate that nsp4 is a key component in DMV assembly and are consistent with nsp4 serving as an anchor or scaffold for the replication complex. Analysis of *cis* and *trans*-acting viral and host factors will further elucidate the processes required for assembly of the coronavirus transcription/replication complex.

Materials and methods

Virus and cell lines

WT-A59 icv, Alb ts6 icv and nsp4-N176A icv were generated using the MHV-A59 reverse genetics system developed by Yount et al. (2002). WT and mutagenized clone B plasmids were transformed into chemically competent MDS (Scarab Genomics) cells. The remaining clones were transformed into chemically competent XL-1 blue cells. Competent cells were heat shocked for 45 s at 42 °C and plated on Luria-Bertani (LB)

plates containing appropriate selection antibiotics. Single colonies were picked and grown in selection media (LB+ antibiotic) overnight at 25 °C. Subcultures of WT and mutant clone B were grown at 37 °C in 350 ml of LB+antibiotic until culture density reached an O.D. of 0.8–1.0 at 590 nm. The remaining clones were treated similarly, but grown at 25 °C. Delayed brain tumor (DBT) and baby hamster kidney (BHK) expressing the MHV receptor (BHK-MHVR) cells were incubated at 37 °C in minimal essential medium, MEM, (Gibco) containing 5% fetal calf serum (FCS), 10% tryptose phosphate broth, 2% penicillin/streptomycin, and 2% L-glutamine. HeLa-MHVR cells were propagated in DMEM (Gibco) containing 10% FCS, 0.001 M sodium *N*-2-hydroxyethylpiperazine-*N*′-2-ethanesulfonic acid, pH 7.4, 1% penicillin/streptomycin and 1% L-glutamine.

Generating infectious clone virus

The coronavirus reverse genetics system described by Yount et al. (2002) was used to generate virus encoding a single amino acid substitution compared to MHV-A59. Primers with two nucleotide changes designed to generate amino acid substitutions at nsp4 positions N176 and N237 to alanine, and N258 to threonine were incorporated into the MHV B plasmid DNA via PCR based site-directed mutagenesis (QuikChange Kit, Stratagene, primers listed in Table 1). Plasmid DNAs containing the specific mutations of interest were isolated and sequenced across the entire B region (sequencing primers shown in Table 1). The B plasmid DNA region of interest was excised and ligated with the MHV A, C, D, E, and F isolated DNA fragments to produce full-length viral cDNA, which was in vitro transcribed using mMessage mMachine T7 kit (Ambion) according to the manufacturer's instructions. Infectious RNA was electroporated into 4×10^6 BHK-MHVR cells and laid over 1.5×10^6 DBT cells in 60 mm dishes in duplicate. Cells were incubated at 33 °C for 24–72 h and monitored for the characteristic cytopathic effect (CPE) of MHV, which is syncytia formation. Supernatant from cultures with CPE was passaged over a fresh monolayer of confluent DBT cells to generate a stock of icv. RNA was isolated from virus-infected cells and subjected to reverse transcriptase (RT)-PCR using primers that flanked the region of interest. PCR amplicons were sequenced to verify the presence of the mutation in infectious clone virus RNA (Fig. 2).

Reverse transcriptase-PCR

The region of viral RNA containing the mutation of interest was RT-PCR amplified using the ImProm-II RT System (Promega) followed by the Advantage cDNA PCR kit (Clonetech) according to the manufacturer's instructions. Specific primers are listed in Table 1.

Determination of nsp4 glycosylation

HeLa-MHVR cells were infected with a recombinant vaccinia virus expressing the bacteriophage T7 polymerase (vTF7.3) at a multiplicity of infection of 10 for 1 h. Then, cells were co-transfected with pPLP2-Cen DNA and either pCen-nsp4 wild type or pCen-nsp4 mutant DNA (N176A, N237A, or N176A/N237A) using Lipofectamine (Gibco) according to the manufacturer's instruction as previously described (Fuerst et al., 1986; Kanjanahaluethai and Baker, 2000). Proteins were radiolabeled with 50 μCi of ^{35}S-*trans*-label from 4.5 to 9.5 h. p.i. Cells were harvested and lysed with lysis buffer A containing 4% SDS, 3% DTT, 40% glycerol and 0.065 M Tris at pH 6.8. Cell lysates were subjected to immunoprecipitation assays as described previously (Schiller et al., 1998). Briefly, radiolabeled cell lysates was diluted in RIPA buffer (0.5% Triton X-100, 0.1% SDS, 300 mM NaCl, 4 mM EDTA and 50 mM Tris–HCl, pH 7.4) and immunoprecipitated with α-nsp4 rabbit antiserum and protein-A sepharose beads (Amersham Biosciences, Piscataway, NJ). For endoglycosidase H (endo H) treatment, protein-A sepharose–antibody–antigen complexes were washed once in RIPA buffer. The endo H treatment was performed according to the manufacturer's instruction (Roche). Briefly, the complexes were resuspended in 20 μl of 50 mM sodium phosphate buffer, pH 6.0, and incubated in the presence and absence of a final concentration of 1 U/μl of endo H for 16 h at 37 °C. The complex-bound sepharose beads were pelleted by centrifugation. The products were eluted from the beads by incubating with 2× Laemmli sample buffer at 37 °C for 30 min. Protein products were separated via electrophoresis on 5–10% gradient SDS-PAGE gels and were visualized by autoradiography.

In tunicamycin treatment experiments, MHV-infected HeLa-MHVR cells were treated with 1 μg/ml tunicamycin (Boehringer Mannheim) for 1 h prior to addition of ^{35}S-*trans*-label, and the drug was present during the 1 h labeling period. Whole cell lysates were prepared and subjected to immunoprecipitation as described above.

Kinetic analysis and temperature shift assays

Viral titer of the WT-A59 icv, Alb ts6 icv, and nsp4-N176A icv was determined via plaque assay. Two sets of DBT cells were infected with WT-A59 icv, Alb ts6 icv, or nsp4-N176A icv at an MOI of 0.1. One set of infected cells was maintained at the permissive temperature of 33 °C, while the other was incubated at the non-permissive temperature of 39.5 °C. At 15 h.p.i. cell-free supernatant was collected. Ten-fold serial dilutions (in triplicate) of isolated supernatant were used to infect DBT cells seeded to 70% confluency in 12 well plates. Following a 1 h absorption period, a 1 ml mixture of 0.4% Noble agar (DIFCO, Detroit, MI) and MEM with 1% FCS and 2% penicillin/streptomycin was added to each well. Infection was maintained for 48 h at the permissive temperature (33 °C) and plates were stained with 0.1% crystal violet solution for 10 min at room temperature to visualize and count plaques.

One-step growth curves were generated by infecting DBT cells at an MOI of 0.1 in 6-well plates. Cells were washed three times with phosphate-buffered saline (PBS) following a 1 h absorption phase. Three milliliters of fresh medium were added and cells were incubated at 33 °C. Aliquots of supernatants were collected 2, 4, 6, 8, 10, and 24 h.p.i. and the viral titer was determined by plaque assay in DBT cells maintained at 33 °C.

Temperature shift growth kinetics were assessed by infecting two sets of DBT cells with WT-A59 icv, Alb ts6 icv, or nsp4-N176A icv at an MOI of 0.1 and incubated at 33 °C. At 6 h.p.i., one set of infected cells was shifted to 39.5 °C. Supernatant was harvested at two hour intervals from 2–14 h.p.i. and virus production was measured by plaque assay in DBT cells maintained at 33 °C.

Statistical analysis of virus kinetics

The logarithm of the titer of each virus (Y) was analyzed using nonlinear regression modeling and the SAS® software package. Since these data clearly exhibit an asymptotic growth pattern, the two-parameter exponential model, $Y=\theta_1(1-\exp\{-\theta_2 x\})+\varepsilon$, was fit to the data using 6 h post infection as the baseline. Separate curves were fitted to each virus and temperature combination; parameter estimates were obtained using maximum likelihood methods, and subsequent tests were performed using likelihood-based F tests (Ratkowsky, 1990).

Immunoprecipitation of cleavage products

Two sets of DBT cells were infected with WT-A59 icv, Alb ts6 icv and nsp4-N176A icv at an MOI of 1.0 and incubated at 33 °C. One hour post infection, actinomycin D (Sigma, St. Louis, MO) was added. At 3.5 h.p.i., cells were grown in media lacking methionine for 30 min. Cells were radiolabeled with ^{35}S-*trans*-label for 2 h at 4 h.p.i. At 4 h.p.i., one set of infected cells was shifted to 39.5 °C. Cell lysates were prepared 6 h.p.i. and subjected to immunoprecipitation with nsp-specific antibodies as described above.

Transmission electron microscopy analysis of DMVs

Two sets of DBT cells were infected with WT-A59 icv or Alb ts6 icv at an MOI of 1.0 and incubated at 33 °C. At 3.5 h.p.i., one set of infected cells was shifted to 39.5 °C. At 5.5 h.p.i., cells were harvested and processed for TEM analysis as previously described (Gosert et al., 2002).

Confocal microscopy

Two sets of DBT or HeLa-MHVR cells were grown to semi-confluence in 8 well chamber slides coated with permanox. Cells were infected with WT-A59 icv or Alb ts6 icv at an MOI of 1.0 and incubated at 33 °C for a 1 h absorption period. At 3.5 h.p.i., one set of infected cells was shifted to 39.5 °C. At 5 h.p.i., cells were labeled with 65 nM MitoTracker Red fluorescent dye (Invitrogen). At 5.5 h.p.i., cells were washed 3 times with PBS and fixed for 30 min at room temperature with 3.7% formaldehyde in PBS. Cells were then permeabilized for 10 min at room temperature with 0.1% Triton X-100 in PBS. Following permeabilization, cells were incubated with either α-nsp3 or α-nsp4 and/or α-PDH antibodies overnight at 4 °C. Cells were then washed 3 times for 30 min in PBS. After washing, cells were incubated with AlexaFluor 488 conjugated chicken α-rabbit IgG (Invitrogen) and/or Alexa Fluor 568 goat α-mouse IgG (Invitrogen) secondary antibody for 30 min at room temperature. Cells were again washed 3 times for 30 min in PBS. Cells were imaged on the Zeiss 510 confocal microscope.

Acknowledgments

We thank Ralph Baric for the generous donation of clones for the reverse genetics system. We also thank Linda Fox of the Loyola Core Imaging Facility for her help with imaging studies, and Katrina Sleeman, Surendranath Baliji, Naina Barretto, Dalia Jukneliene, and other members of the Baker lab for their technical assistance and suggestions. This research was supported by Public Health Service Research Grant AI 45798.

References

Baker, S.C., Shieh, C.K., Soe, L.H., Chang, M.F., Vannier, D.M., Lai, M.M., 1989. Identification of a domain required for autoproteolytic cleavage of murine coronavirus gene A polyprotein. J. Virol. 63 (9), 3693–3699.

Baker, S.C., Denison, M.R., 2008. Cell biology of nidovirus replication complexes. In: Perlman, S., Gallagher, T., Snijder, E. (Eds.), Nidoviruses. ASM Press, Washington, pp. 103–113.

Baric, R.S., Fu, K., Schaad, M.C., Stohlman, S.A., 1990. Establishing a genetic recombination map for murine coronavirus strain A59 complementation groups. Virology 177 (2), 646–656.

Bonilla, P.J., Hughes, S.A., Weiss, S.R., 1997. Characterization of a second cleavage site and demonstration of activity in *trans* by the papain-like proteinase of the murine coronavirus mouse hepatitis virus strain A59. J. Virol. 71 (2), 900–909.

Bost, A.G., Carnahan, R.H., Lu, X.T., Denison, M.R., 2000. Four proteins processed from the replicase gene polyprotein of mouse hepatitis virus colocalize in the cell periphery and adjacent to sites of virion assembly. J. Virol. 74 (7), 3379–3387.

Deming, D.J., Graham, R.L., Denison, M.R., Baric, R.S., 2007. Processing of open reading frame 1a replicase proteins nsp7 to nsp10 in murine hepatitis virus strain A59 replication. J. Virol. 81 (19), 10280–10291.

Denison, M.R., Hughes, S.A., Weiss, S.R., 1995. Identification and characterization of a 65-kDa protein processed from the gene 1 polyprotein of the murine coronavirus MHV-A59. Virology 207 (1), 316–320.

Donaldson, E.F., Graham, R.L., Sims, A.C., Denison, M.R., Baric, R.S., 2007. Analysis of murine hepatitis virus strain A59 temperature-sensitive mutant TS-LA6 suggests that nsp10 plays a critical role in polyprotein processing. J. Virol. 81 (13), 7086–7098.

Fu, K., Baric, R.S., 1994. Map locations of mouse hepatitis virus temperature-sensitive mutants: confirmation of variable rates of recombination. J. Virol. 68 (11), 7458–7466.

Fuerst, T.R., Niles, E.G., Studier, F.W., Moss, B., 1986. Eukaryotic transient-expression system based on recombinant vaccinia virus that synthesizes bacteriophage T7 RNA polymerase. Proc. Natl. Acad. Sci. U. S. A. 83 (21), 8122–8126.

Goldsmith, C.S., Tatti, K.M., Ksiazek, T.G., Rollin, P.E., Comer, J.A., Lee, W.W., Rota, P.A., Bankamp, B., Bellini, W.J., Zaki, S.R., 2004. Ultrastructural characterization of SARS coronavirus. Emerg. Infect. Dis. 10 (2), 320–326.

Gosert, R., Kanjanahaluethai, A., Egger, D., Bienz, K., Baker, S.C., 2002. RNA replication of mouse hepatitis virus takes place at double-membrane vesicles. J. Virol. 76 (8), 3697–3708.

Graham, R.L., Denison, M.R., 2006. Replication of murine hepatitis virus is regulated by papain-like proteinase 1 processing of nonstructural proteins 1, 2, and 3. J. Virol. 80 (23), 11610–11620.

Harcourt, B.H., Jukneliene, D., Kanjanahaluethai, A., Bechill, J., Severson, K.M., Smith, C.M., Rota, P.A., Baker, S.C., 2004. Identification of severe acute respiratory syndrome coronavirus replicase products and characterization of papain-like protease activity. J. Virol. 78 (24), 13600–13612.

Kanjanahaluethai, A., Baker, S.C., 2000. Identification of mouse hepatitis virus papain-like proteinase 2 activity. J. Virol. 74 (17), 7911–7921.

Kanjanahaluethai, A., Baker, S.C., 2001. Processing of the replicase of murine coronavirus: papain-like proteinase 2 (PLP2) acts to generate p150 and p44. Adv. Exp. Med. Biol. 494, 267–273.

Kanjanahaluethai, A., Jukneliene, D., Baker, S.C., 2003. Identification of the murine coronavirus MP1 cleavage site recognized by papain-like proteinase 2. J. Virol. 77 (13), 7376–7382.

Kanjanahaluethai, A., Chen, Z., Jukneliene, D., Baker, S.C., 2007. Membrane topology of murine coronavirus replicase nonstructural protein 3. Virology 361 (2), 391–401.

Kopek, B.G., Perkins, G., Miller, D.J., Ellisman, M.H., Ahlquist, P., 2007. Three-dimensional analysis of a viral RNA replication complex reveals a virus-induced mini-organelle. PLoS Biol. 5 (9), e220.

Lu, Y., Lu, X., Denison, M.R., 1995. Identification and characterization of a serine-like proteinase of the murine coronavirus MHV-A59. J. Virol. 69 (6), 3554–3559.

Lu, X.T., Sims, A.C., Denison, M.R., 1998. Mouse hepatitis virus 3C-like protease cleaves a 22-kilodalton protein from the open reading frame 1a polyprotein in virus-infected cells and in vitro. J. Virol. 72 (3), 2265–2271.

Masters, P.S., 2006. The molecular biology of coronaviruses. Adv. Virus Res. 66, 193–292.

Miller, D.J., Ahlquist, P., 2002. Flock house virus RNA polymerase is a transmembrane protein with amino-terminal sequences sufficient for mitochondrial localization and membrane insertion. J. Virol. 76 (19), 9856–9867.

Miller, D.J., Schwartz, M.D., Ahlquist, P., 2001. Flock house virus RNA replicates on outer mitochondrial membranes in *Drosophila* cells. J. Virol. 75 (23), 11664–11676.

Miller, D.J., Schwartz, M.D., Dye, B.T., Ahlquist, P., 2003. Engineered retargeting of viral RNA replication complexes to an alternative intracellular membrane. J. Virol. 77 (22), 12193–12202.

Oostra, M., Te Lintelo, E.G., Deijs, M., Verheije, M.H., Rottier, P.J., de Haan, C.A., 2007. Localization and membrane topology of the coronavirus nonstructural protein 4: involvement of the early secretory pathway in replication. J. Virol. 81 (22), 12323–12336.

Peiris, J.S., Guan, Y., Yuen, K.Y., 2004. Severe acute respiratory syndrome. Nat. Med. 10 (12 Suppl), S88–S97.

Prentice, E., Jerome, W.G., Yoshimori, T., Mizushima, N., Denison, M.R., 2004. Coronavirus replication complex formation utilizes components of cellular autophagy. J. Biol. Chem. 279 (11), 10136–10141.

Ratkowsky, D., 1990. "Handbook of Nonlinear Regression Models." Marcel Dekker, New York.

Salonen, A., Ahola, T., Kaariainen, L., 2005. Viral RNA replication in association with cellular membranes. Curr. Top. Microbiol. Immunol. 285, 139–173.

Sawicki, S.G., Sawicki, D.L., Younker, D., Meyer, Y., Thiel, V., Stokes, H., Siddell, S.G., 2005. Functional and genetic analysis of coronavirus replicase–transcriptase proteins. PLoS Pathog. 1 (4), e39.

Sawicki, S.G., Sawicki, D.L., Siddell, S.G., 2007. A contemporary view of coronavirus transcription. J. Virol. 81 (1), 20–29.

Schaad, M.C., Stohlman, S.A., Egbert, J., Lum, K., Fu, K., Wei Jr., T., Baric, R.S., 1990. Genetics of mouse hepatitis virus transcription: identification of cistrons which may function in positive and negative strand RNA synthesis. Virology 177 (2), 634–645.

Schiller, J.J., Kanjanahaluethai, A., Baker, S.C., 1998. Processing of the coronavirus MHV-JHM polymerase polyprotein: identification of precursors and proteolytic products spanning 400 kilodaltons of ORF1a. Virology 242 (2), 288–302.

Shi, S.T., Schiller, J.J., Kanjanahaluethai, A., Baker, S.C., Oh, J.W., Lai, M.M., 1999. Colocalization and membrane association of murine hepatitis virus gene 1 products and de novo-synthesized viral RNA in infected cells. J. Virol. 73 (7), 5957–5969.

Siddell, S., Sawicki, D., Meyer, Y., Thiel, V., Sawicki, S., 2001. Identification of the mutations responsible for the phenotype of three MHV RNA-negative ts mutants. Adv. Exp. Med. Biol. 494, 453–458.

Snijder, E.J., van der Meer, Y., Zevenhoven-Dobbe, J., Onderwater, J.J., van der Meulen, J., Koerten, H.K., Mommaas, A.M., 2006. Ultrastructure and origin of membrane vesicles associated with the severe acute respiratory syndrome coronavirus replication complex. J. Virol. 80 (12), 5927–5940.

Sparks, J.S., Lu, X., Denison, M.R., 2007. Genetic analysis of murine hepatitis virus nsp4 in virus replication. J. Virol. 81 (22), 12554–12563.

Stadler, K., Masignani, V., Eickmann, M., Becker, S., Abrignani, S., Klenk, H.D., Rappuoli, R., 2003. SARS—beginning to understand a new virus. Nat. Rev. Microbiol. 1 (3), 209–218.

Younker, D.R., Sawicki, S.G., 1998. Negative strand RNA synthesis by temperature-sensitive mutants of mouse hepatitis virus. Adv. Exp. Med. Biol. 440, 221–226.

Yount, B., Denison, M.R., Weiss, S.R., Baric, R.S., 2002. Systematic assembly of a full-length infectious cDNA of mouse hepatitis virus strain A59. J. Virol. 76 (21), 11065–11078.

Ziebuhr, J., Snijder, E.J., 2007. The coronavirus replicase gene: special enzymes for special viruses. In: Thiel, V. (Ed.), "Coronaviruses: Molecular and Cellular Biology". Caister Academic Press.

Ziebuhr, J., Snijder, E.J., Gorbalenya, A.E., 2000. Virus-encoded proteinases and proteolytic processing in the Nidovirales. J. Gen. Virol. 81 (Pt 4), 853–879.